The mouse homeobox gene *Not* is required for caudal notochord development and affected by the truncate mutation

Hanaa Ben Abdelkhalek,[1,5] Anja Beckers,[1,5] Karin Schuster-Gossler,[1,5] Maria N. Pavlova,[1,6] Hannelore Burkhardt,[1] Heiko Lickert,[2] Janet Rossant,[2] Richard Reinhardt,[3] Leonard C. Schalkwyk,[3,7] Ines Müller,[3] Bernhard G. Herrmann,[3] Marcelo Ceolin,[4,8] Rolando Rivera-Pomar,[4,9] and Achim Gossler[1,10]

[1]Institute for Molecular Biology OE5250, Medizinische Hochschule Hannover, D-30625 Hannover, Germany; [2]Samuel Lunenfeld Research Institute, Mount Sinai Hospital, Toronto M5G 1X5, Ontario, Canada; [3]Max-Planck-Institute for Molecular Genetics, D-14195 Berlin, Germany; [4]Max-Planck-Institute for Biophysical Chemistry, D-37077 Göttingen, Germany

The floating head (*flh*) gene in zebrafish encodes a homeodomain protein, which is essential for notochord formation along the entire body axis. *flh* orthologs, termed *Not* genes, have been isolated from chick and *Xenopus*, but no mammalian ortholog has yet been identified. Truncate (*tc*) is an autosomal recessive mutation in mouse that specifically disrupts the development of the caudal notochord. Here, we demonstrate that truncate arose by a mutation in the mouse *Not* gene. The truncate allele (Not^{tc}) contains a point mutation in the homeobox of *Not* that changes a conserved Phenylalanine residue in helix 1 to a Cysteine (F20C), and significantly destabilizes the homeodomain. Reversion of F20C in one allele of homozygous *tc* embryonic stem (ES) cells is sufficient to restore normal notochord formation in completely ES cell-derived embryos. We have generated a targeted mutation of *Not* by replacing most of the *Not* coding sequence, including the homeobox with the *eGFP* gene. The phenotype of $Not^{eGFP/eGFP}$, $Not^{eGFP/tc}$, and $Not^{tc/tc}$ embryos is very similar but slightly more severe in $Not^{eGFP/eGFP}$ than in $Not^{tc/tc}$ embryos. This confirms allelism of truncate and *Not*, and indicates that *tc* is not a complete null allele. *Not* expression is abolished in *Foxa2* and *T* mutant embryos, suggesting that *Not* acts downstream of both genes during notochord development. This is in contrast to zebrafish embryos, in which *flh* interacts with *ntl* (zebrafish *T*) in a regulatory loop and is essential for development of the entire notochord, and suggests that different genetic control circuits act in different vertebrate species during notochord formation.

[*Keywords*: Notochord development; *Not* gene; homeodomain protein]

Received March 22, 2004; revised version accepted May 13, 2004.

Chordate embryos are characterized by a rod-like structure, the notochord, which is located ventral to the neural tube in the midline of the embryo. In vertebrate embryos, the notochord is essential for dorsoventral patterning of the paraxial mesoderm and neural tube. Mutations disrupting notochord development, or experimental removal of the notochord, prevent sclerotome differentiation in the somites and floorplate induction in the spinal cord (van Straaten and Hekking 1991; Yamada et al. 1991). Conversely, grafts of notochord into presomitic mesoderm laterally to the neural tube suppresses dermomyotome formation and induces ectopic sclerotome (Pourquié et al. 1993) as well as a supernumerary ectopic floorplate (van Straaten et al. 1985; Placzek et al. 1990). Thus, the notochord is both necessary and sufficient for the induction of ventral cell fates in the paraxial mesoderm and neural tube. The ventralizing signals of the notochord are mediated by sonic hedge-

[5]These authors contributed equally to this work.
Present addresses: [6]Nura Inc., 1124 Columbia St., Seattle, WA 98104, USA; [7]Institute of Psychiatry, Box P082, De Crespigny Park, London SE5 8AF, UK; [8]Centro Regional de Estudios Genomicos, Laboratorio de Biofisica Molecular y Proteomica, Av. Calchaqui Km 23,5, 1888 Florencio Varela, Argentina; [9]Centro Regional de Estudios Genomicos (CREG), Universidad Nacional de La Plata, Calle 7 No 776, 1900 La Plata, Argentina.
[10]Corresponding author.
E-MAIL Gossler.Achim@mh-hannover.de; FAX 49-511-532-4283.
Article published online ahead of print. Article and publication date are at http://www.genesdev.org/cgi/doi/10.1101/gad.303504.

hog (Shh; Bumcrot and McMahon 1995) a vertebrate homolog of the *Drosophila* segment polarity gene Hedgehog, which is expressed in the notochord and floor plate (Echelard et al. 1993) and can substitute for the ventralizing effects of the notochord in a variety of experimental conditions.

Notochord cells are generated during gastrulation from axial mesendodermal cells that migrate through the node (Lawson et al. 1991; Selleck and Stern 1991; Lawson and Pedersen 1992; Tam et al. 1997; Kinder et al. 2001), and during subsequent development from the tail bud (Schoenwolf 1984; Wilson and Beddington 1996). Whereas the functional significance of the notochord is well established, few genes that control notochord development in vertebrate embryos are known. In the mouse, two genes, *T* and *Foxa2*, that encode transcription factors and are pivotal for notochord formation, have been identified by positional cloning and targeted mutagenesis, respectively (Herrmann et al. 1990; Ang and Rossant 1994; Weinstein et al. 1994). Homozygous *T* mutant embryos lack a node and trunk notochord, but have notochord cells in the head process (Herrmann 1995), whereas *Foxa2* mutant embryos do not form a node and lack all notochord cells (Ang and Rossant 1994; Weinstein et al. 1994). Another transcription-factor encoding gene, *flh*, which is essential for notochord formation and acts upstream of *T* in notochord precursors was identified in zebrafish (Talbot et al. 1995). Similar to *T* mutants, homozygous *flh* mutant embryos form a prechordal plate but lack a differentiated notochord (Talbot et al. 1995). *flh* orthologs, termed *Not* genes, were identified in chick and *Xenopus*, but no mammalian *Not* gene has been identified thus far.

In mice, several mutations that specifically affect the development of the notochord have been identified (for review, see Theiler 1988). One of these, truncate (*tc*), is a recessive mutation with variable expressivity and incomplete penetrance that specifically affects the development of the caudal notochord (Theiler 1959; Dietrich et al. 1993). In homozygous *tc* embryos, notochord formation is normal until around embryonic day 9.5 (E9.5), but comes to an abrupt halt shortly later, leading to defects in the axial skeleton posterior to the lumbar region (Theiler 1959; Dietrich et al. 1993). As a prerequisite for cloning the gene affected by the *tc* mutation, we have previously generated a fine genetic map of the *tc* region (Pavlova et al. 1998). Here, we report that *tc* affects the mouse *Not* gene. The *tc* allele carries a point mutation in helix 1 of the homeobox that destabilizes the homeodomain. Truncate represents a strong hypomorphic allele of *Not* as indicated by very similar phenotypes of embryos homozygous for the *tc* allele and for a targeted null mutation that we generated. No *Not* expression was detected in *Foxa2* or *T* mutant embryos, suggesting that *Not* acts downstream of both genes. Our results suggest that in contrast to zebrafish in mouse embryos, development of the anterior notochord is independent of *Not* function.

Results

Identification of Not *as a candidate gene affected by the truncate mutation*

Previously, we had delineated by fine genetic mapping, the critical interval containing *tc* between the markers *D6R4Arb5* and *D6Mit6* (Pavlova et al. 1998). Using these markers as probes, we isolated BAC clones and initiated a chromosomal walk. *D6Mit6* identified among others BAC 379-N23, whose Sp6 end detected the same recombinant haplotypes as *D6Mit6*, whereas a probe from the T7 end detected only the *tc*-specific haplotype in all relevant back-cross DNAs. This indicated that the T7 end of 379-N23 was closer to *tc*, and placed all distal recombination breakpoints in the region covered by this BAC clone (Fig. 1A). Using the T7 end of BAC 379-N23 as probe, additional BAC clones were isolated. The Sp6 end of one of these clones, 179f16, overlapped with 379-N23, whereas a probe from the 179f16 T7 end detected recombinant haplotypes in two back-cross DNAs, indicating that the *tc* interval was contained within the overlapping BACs 379-N23 and 179f16. Further analyses of these and other BAC clones reduced the interval to ~180 kb. This region was completely sequenced, and known and predicted genes in this region were identified by computational analysis. One of the predicted genes encoded a protein of 240 amino acids containing a homeodomain of the *ems* subfamily, which includes zebrafish *flh* (Talbot et al. 1995), *Cnot1*, *Cnot2* (Stein and Kessel 1995; Stein et al. 1996), *Xnot1*, and *Xnot2* (Gont et al. 1993; von Dassow et al. 1993). Because these genes are specifically expressed in the notochord and *flh* is essential for notochord formation in zebrafish embryos (Talbot et al. 1995), this mouse gene, hereafter referred to as *Not*, represented an appealing candidate for *tc* and was analyzed further. A cDNA covering the three predicted exons of *Not* (Fig. 1B), was isolated by RT–PCR from mRNA of day 9.5 embryos. Comparison of the cDNA with the genomic sequence confirmed the predicted exon/intron structure, which is highly similar to chicken *Cnot2* (Stein et al. 1996). The homeodomain of mouse *Not* shares 56%–60% identity with the homeodomains of the chicken, *Xenopus*, and zebrafish genes (Fig. 1C), the most closely related vertebrate *Not* genes being *Cnot2* and ZF *flh* (Fig. 1D). Sequence conservation does not extend into regions outside of the homeodomain.

Expression of Not

Expression of *Not* in wild-type embryos was analyzed by whole-mount in situ hybridization using probes derived from the cDNA. No *Not* transcripts were detected in E6.5 embryos prior to the formation of the primitive streak and the onset of gastrulation (data not shown). At the extended primitive streak stage on E7.5, *Not* transcripts were detected in the node at the distal tip of the egg cylinder (Fig. 2a) and were largely confined to the ventral node (Fig. 2h,i). Between E8 and E9, *Not* transcripts were abundant in the node and newly formed notochord, whereas more anterior, older notochord

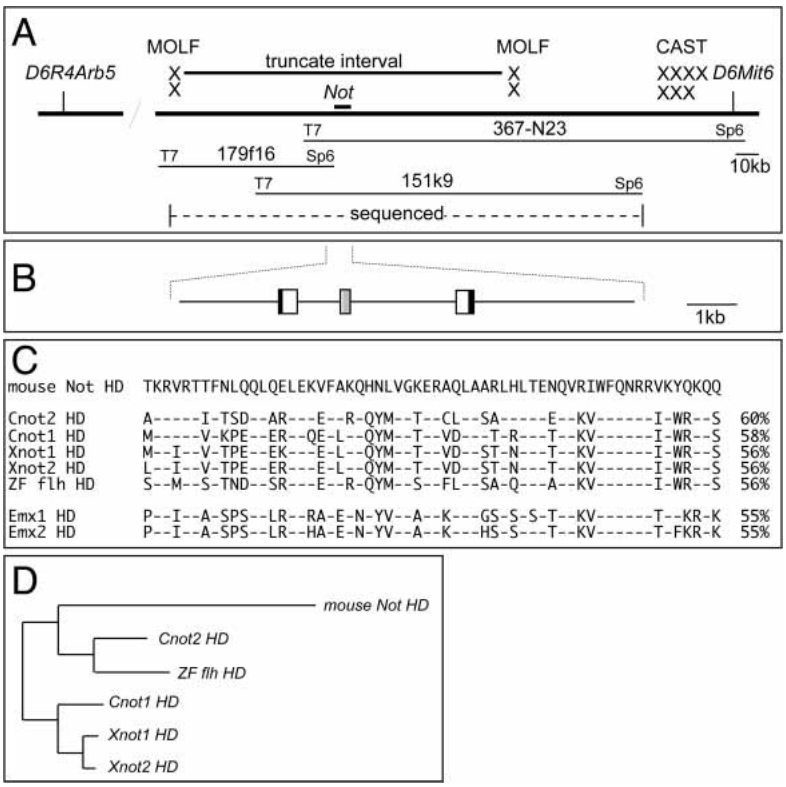

Figure 1. *Not* localization, structure, and similarity to other vertebrate *Not* genes. (*A*) Physical map of the truncate region. The position and number of recombination breakpoints that were obtained in MOLF and CAST back-cross animals is indicated by ×s *above* the map, relevant BAC clones are shown *below*. (*B*) Structure of the *Not* gene. Boxes indicate exons. Black and white filling represents noncoding and coding regions, respectively. The homeobox is hatched. (*C*) Alignment of the homeodomains of mouse, chick, *Xenopus*, and zebrafish *Not*, and mouse *Emx1* and *Emx2* genes. The percentage of identical amino acids is indicated to the *right*. (*D*) Midpoint rooted phylogenetic tree of vertebrate *Not* genes based on ClustalW aligned homeodomains.

showed no expression (Fig. 2b–d). During subsequent development until E12.5, *Not* expression was confined to the notochordal plate and caudal portion of the notochord (Fig. 2e–g). No *Not* transcripts were detected in E13.5 embryos (data not shown). Thus, *Not* expression is restricted to the node and notochord cells during gastrulation and axis elongation, closely resembling *Not* gene expression in the axial mesoderm of zebrafish, *Xenopus*, and chick embryos (von Dassow et al. 1993; Stein and Kessel 1995; Talbot et al. 1995; Melby et al. 1997). *Not* transcripts were also detected in the node and posterior notochord of homozygous *tc* embryos at levels similar to wild type (Fig. 2k–n; data not shown). In contrast to wild-type embryos, *Not* transcripts persisted temporarily at high levels in the head process and anterior notochord of mutant E8 and E8.25 embryos (Fig. 2k,l). Similarly, at later stages, expression extended further anterior than in wild-type embryos (Fig. 2m,n), suggesting that down-regulation in the notochord was delayed. In older stages, *Not* expression in the posterior notochord of truncate mutant embryos was discontinuous and reflected the loss or disruptions of the notochord (arrowhead in Fig. 2n).

The tc *allele of* Not *contains a point mutation in the homeobox that affects homeodomain stability*

Apparently normal expression levels of *Not* in *tc* mutant embryos suggested that the *tc* phenotype is not due to reduced *Not* transcription. To identify potential mutations in the coding region of *Not* in *tc* mutants, the three exons were amplified by PCR from genomic DNA of two homozygous *tc* mice, and from DNA of C57BL/6, 129Sv/ImJ, FVB/N, and CD1 wild-type mice, subcloned, and sequenced. Exon/intron junctions and exons one and three of wild-type and mutant DNAs were identical. A single base change (T → G) was identified in six independent clones containing exon two from different mutant DNAs (Fig. 3A). This base change leads to a substitution of Phenylalanine by Cysteine in position 20 of helix 1 of the homeodomain (F20C). To address whether the F20C mutation leads to the *tc* phenotype, we generated $Not^{tc/tc}$ embryonic stem (ES) cells, and corrected the F20C mutation in one *Not* allele of these cells by homologous recombination using a replacement vector that contained the wild-type exon 2 sequence in its 5′ region of homology (Fig. 3C). The selection cassette was removed by transient expression of Cre in correctly targeted cells. The reversion to wild type (*tcrev*) was verified by cloning and sequencing exon 2 from the targeted allele. $Not^{tc/tc}$, and $Not^{tc/tcrev}$ ES cells were used to generate completely ES-derived embryos by injection of tetraploid morulae (Nagy et al. 1990). Two of eleven completely $Not^{tc/tc}$ ES cell-derived E11–E11.5 embryos showed disruptions in the notochord characteristic for *tc* mutant embryos (Fig. 3E, panels b,c,g,h). This low frequency most likely reflects the incomplete penetrance and highly variable expressivity of the *tc* phenotype, which is also observed in *Not* null mutant embryos that we generated (see below). In contrast, none of 35 embryos obtained with $Not^{tc/tcrev}$ ES cells either with ($n = 20$) or without ($n = 15$) the puro cassette showed

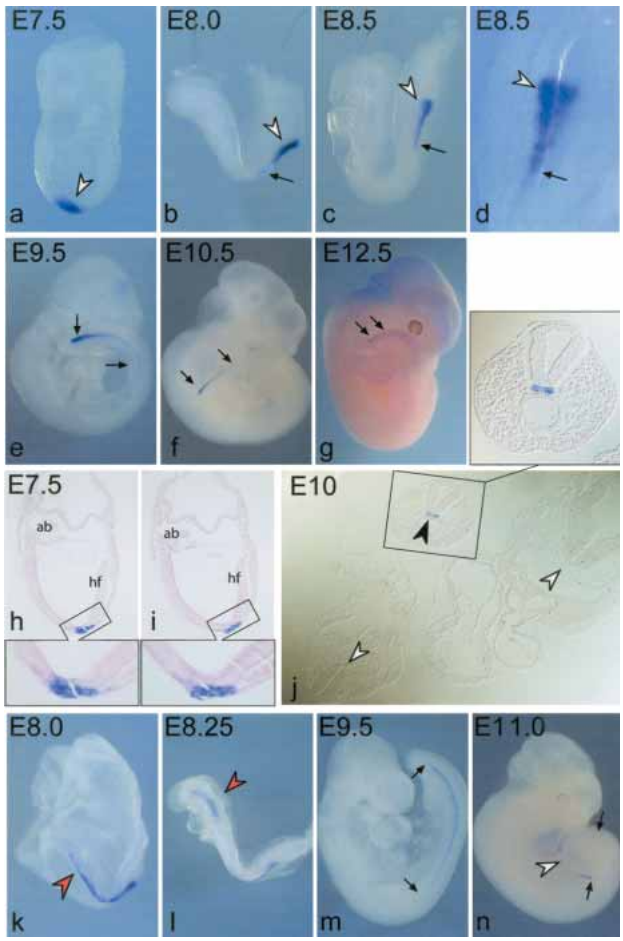

Figure 2. Expression of *Not* during embryonic development. Wild-type (*a–g*) and homozygous truncate (*k–n*) embryos and sections of wild-type (*h–j*) embryos after whole-mount in situ hybridization with a *Not* cDNA probe. Expression in wild-type embryos was first detected in the node, and was subsequently restricted to the node (arrowheads in *a–d*) and caudal portions of the notochord (arrows in *b–g*). (*h*,*i*) Sections of a hybridized day 7.5 embryo. The boxed regions showing the node in *h* and *i* are enlarged *below*. (*j*) Section of a day 10 embryo showing restriction of *Not* transcripts to the caudal notochord. No other expression domains were detected. White arrowheads in *j* point to the notochord in nonexpressing regions, the black arrowhead indicates the caudal *Not*-expressing notochord. In truncate embryos, ectopic transcripts were detected in the head process and anterior notochord (red arrowheads in *k*,*l*) of mutant day 8 and 8.25 embryos. Subsequently, the expression domain in the notochord (arrows in *m*,*n*) appeared extended. The arrowhead in *n* points to a gap in the notochord reflecting the *tc* phenotype. (ab) Allantoic bud; (hf) headfold.

disruptions of the notochord (Fig. 3E, panels d,e,i,j; data not shown), strongly suggesting that the F20C mutation is responsible for the notochord defects in *tc* mutant embryos.

Phenylalanine 20 is conserved in vertebrate *Not* genes (Fig. 1C). In homeodomains of other homeobox genes, a Phenylalanine residue or another hydrophobic amino acid is found in this position (http://www.sanger.ac.uk/cgi-bin/Pfam/getalignment.pl?name=homeobox&acc=PF00046&format=link; examples in Fig. 3B). This suggested that the substitution of phenylalanine by Cysteine could affect the biochemical or physicochemical properties of the homeodomain. To analyze the effect of the F20C mutation on the Not homeodomain, we expressed the wild-type and mutant Not homeodomain as GST fusion proteins, and measured the circular dicroism and determined the thermal denaturation curve of the purified wild-type and truncate Not homeodomains. The pattern of circular dichroism of the wild-type and mutant protein in the far UV was equivalent at 25°C (Fig. 3F), and similar to that observed for other homeodomains (Ades and Sauer 1994; Subramaniam et al. 2001), indicating that the helical structure of the Not homeodomain is not altered by the F20C change. However, measuring the helical content of the homeodomains as a function of the temperature showed that the F20C mutation caused a significant destabilization of the Not homeodomain in vitro (Fig. 3G) that could impact on *Not* function in vivo.

tc *is a strong hypomorphic allele*

Null alleles of *flh* in zebrafish cause the complete absence of the notochord (Halpern et al. 1995; Talbot et al. 1995), whereas in *tc* mutants, only the posterior notochord is affected. Thus, *Not* function in mouse is either dispensable for anterior notochord development or *tc* represents a hypomorphic allele sufficient for anterior but not posterior notochord development. To determine the nature of the truncate allele and to determine the consequences of a complete loss of *Not* function, we generated a targeted mutation of *Not*. We inserted *eGFP* in frame into the endogenous ORF in exon 1, and deleted most of exon 1 and the complete exon 2, thereby removing ~80% of the predicted ORF, including most of the homeodomain (Fig. 4 A). This should place *eGFP* expression under the regulatory control of the *Not* promoter and prevent the generation of a truncated *Not* protein. Germ-line chimeras with two independent correctly targeted ES cell clones were generated, and isogenic $Not^{eGFPneo}$ mice on a 129Sv/ImJ background were established. The neo cassette was removed by passing the targeted allele through the germ line of ZP3::Cre females (de Vries et al. 2000) of back-cross generation N6 to 129Sv/ImJ.

Heterozygous mice carrying the Not^{eGFP} allele appeared normal (Fig. 4C), and $Not^{eGFP/+}$ embryos expressed eGFP in the caudal notochord closely resembling the distribution of *Not* transcripts (Fig. 5A). Heteroallelic $Not^{tc/eGFP}$ mice (Fig. 4C) displayed with incomplete penetrance and variable expressivity, tail and axial skeleton defects similar to truncate mice, indicating that Not^{eGFP} disrupts *Not* function, and proving that *tc* is a *Not* allele. Homozygous Not^{eGFP} null mutants also showed vertebral column defects and caudal agenesis of varying severity that were confined to the tail and the sacral region (Fig. 4C; data not shown). Homozygous Not^{tc} mice are viable, but viability is reduced, which was attributed at

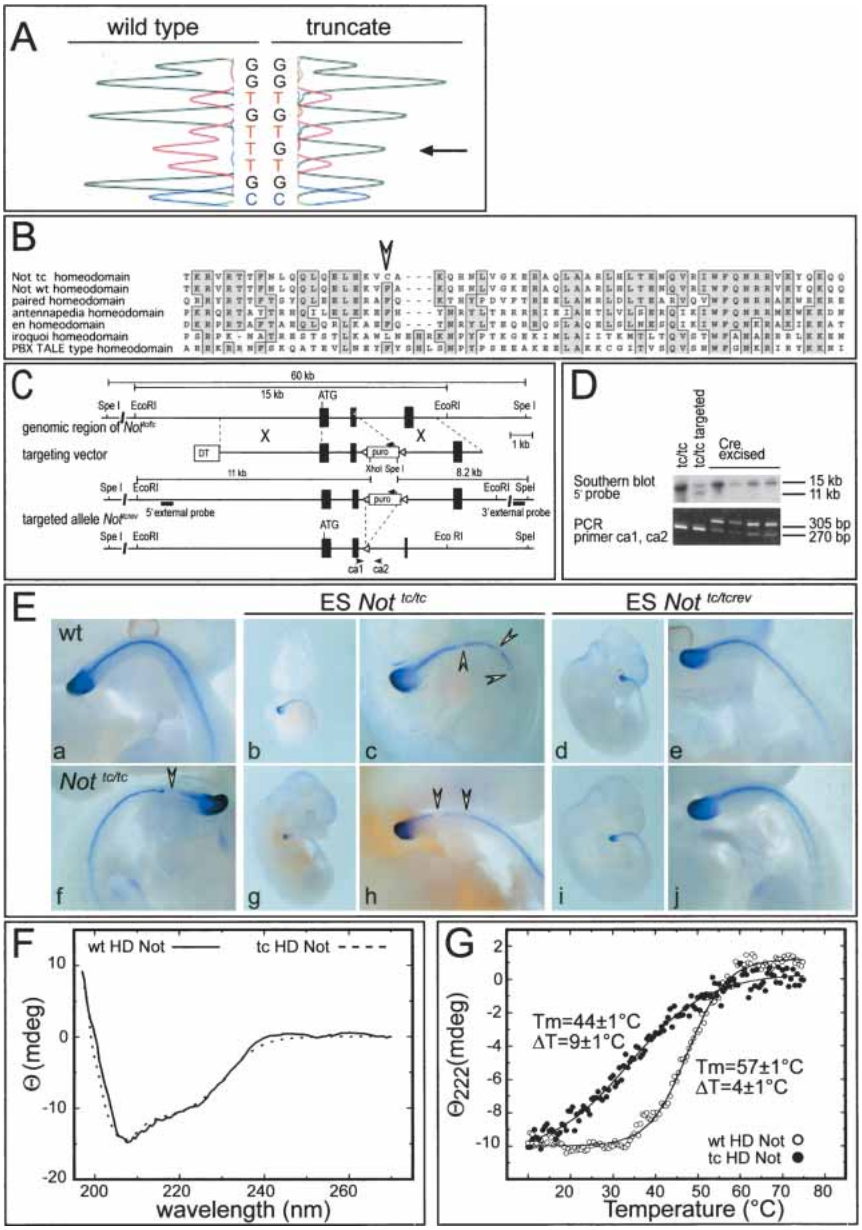

Figure 3. A point mutation in helix 1 of the homeodomain affects stability. (*A*) Partial nucleotide sequence of the wild-type and truncate *Not* allele around the T → G mutation. (*B*) Amino acid alignment of various homeodomains. An arrowhead indicates the position of the changed amino acid in Not^{tc}. (*C*) Targeting strategy for reverting F20C. Exons are indicated by black boxes, relevant restriction sites and restriction fragments, as well as the probes used for genotyping, are shown *above* and *below*. The asterisk in exon 2 of the genomic locus indicates the point mutation. (*D*) Southern blot and PCR analysis of targeted clones after Cre-mediated excision of puro, using the primers ca1 and ca2 indicated in *C*. (*E*) Glycerol cleared wild-type (wt; panel *a*) and $Not^{tc/tc}$ (panel *f*) embryos collected from natural matings, and completely ES cell-derived embryos obtained with $Not^{tc/tc}$ (panels *b*,*c*,*g*,*h*) and $Not^{tc/tcrev}$ (panels *d*,*e*,*i*,*j*) cells, respectively, after in situ hybridization with a brachyury probe. Panels *c*, *e*, *h*, and *j* show higher magnifications of the embryos shown in panels *b*, *d*, *g*, and *i*. Arrowheads in panels *c*, *f*, and *h* point to gaps in the notochords. (*F*) UV-CD spectra obtained from HD NOT1-WT (solid line) and HD-NOT1-F20C (broken line). (*G*) Thermal denaturation curves obtained from HD NOT1-WT (open circles) and HD-NOT1-F20C (filled circles) monitored by the ellipticity of the absorption signal at 222 nm indicate a significant reduction of the melting temperature of HD-Not F20C (≈44°C compared with 57°C of the wild-type homeodomain).

least in part to spinal injury in the sacral and lower lumbar region (Theiler 1959). Homozygous Not^{eGFP} mice were obtained from heterozygous matings at birth with a Mendelian ratio. However, only ~20% of the homozygotes survived until weaning. Dead mutants that were recovered before weaning had short tail stumps or no tails and may represent the most severe manifestation of loss of *Not* function, whereas most of the survivors had apparently normal tails or minor skeletal defects (Fig. 4C). Defective notochord development and axial truncations can be associated with kidney defects and other urogenital and anorectal malformations that cause postnatal lethality (Gluecksohn-Schoenheimer 1943; Berry 1960). Such defects are unlikely to account for the high postnatal mortality, as homozygous E18.5 Not^{GFP} fetuses (n = 12) and recovered dead newborns (n = 10) had apparently normal kidneys and no obvious anorectal malformations. Whether other organ defects contribute to the high mortality requires further analyses. Also, homozygous E11.5 and 13.5 Not^{eGFP} embryos were phenotypically similar to double heterozygous $Not^{tc/eGFP}$ or homozygous $Not1^{tc}$ embryos (Fig. 5B), and showed variable defects typical for truncate mutants, such as thin or constricted tails (white arrowheads in Fig. 5B), premature ending of the notochord in and caudal to the sacral region (arrows in Fig. 5B), and a discontinuous caudal notochord with scattered displaced remnants (arrowheads in Fig. 5B). To address at which axial level notochord development was affected, the notochord of homozygous E9.5 and 10.5 Not^{eGFP} and Not^{tc} embryos was visualized by in situ hybridization with a brachyury probe. In E9.5 $Not^{eGFP/eGFP}$ (n = 13) and $Not^{tc/tc}$ (n = 7)

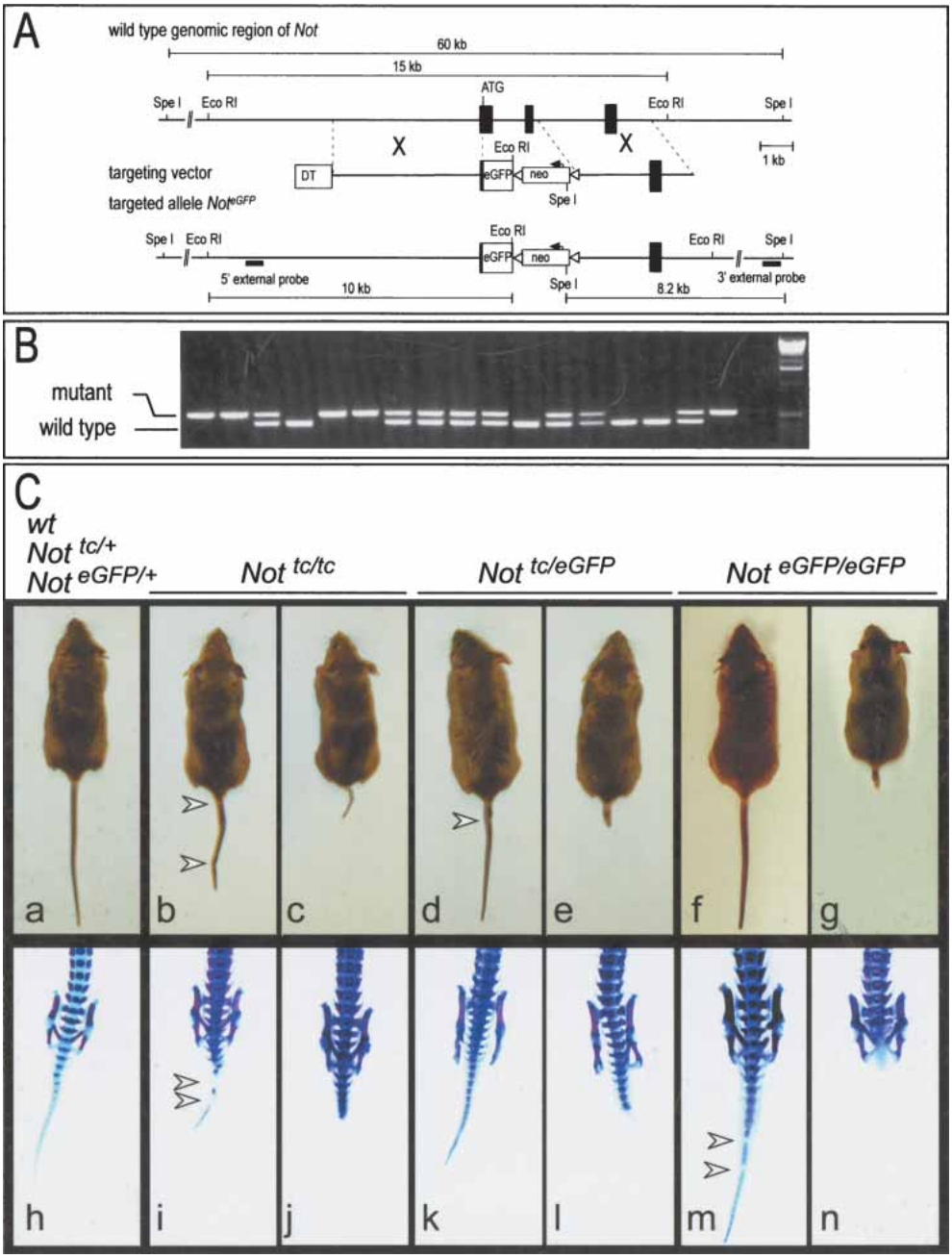

Figure 4. Gene targeting strategy and external and skeletal phenotypes of *Not* mutant mice. (*A*) Schematic representation of the genomic locus, targeting vector, and mutated allele. Exons are indicated by black boxes, relevant restriction sites and restriction fragments, as well as the probes used for genotyping are shown above and below. (*B*) Genotyping PCR on genomic DNA from newborns (two litters) derived from matings of $Not^{eGFP/+}$ mice. (*C*) Representative examples of external adult phenotypes and skeletal preparations of $Not^{tc/tc}$, $Not^{eGFP/tc}$, and $Not^{eGFP/eGFP}$ newborn mice. Arrowheads point to constrictions in the tails and gaps in vertebrae, respectively.

embryos, no defects in the notochord were observed (Fig. 5C, panels b,c; data not shown). On E10.5, two of six $Not^{tc/tc}$ embryos showed notochord defects posterior to the hindlimb buds (Fig. 5C, panel g; data not shown). More anterior defects were observed in the notochords of two of nine homozygous Not^{GFP} embryos (Fig. 5C, panel h), whereas all other embryos had essentially normal notochords along the entire axis or minor posterior defects (Fig. 5C, panel f; data not shown). The anteriormost disruption of the notochord found in these embryos was caudal to somite 16/17 (Fig. 5C, panel h; data not shown), and was thus about five somites more cranial than notochord defects in truncate embryos (Theiler 1959, 1988). Increased postnatal lethality, higher penetrance of caudal truncations, and slightly more anterior disruption of notochord development in Not^{eGFP} null mice suggest

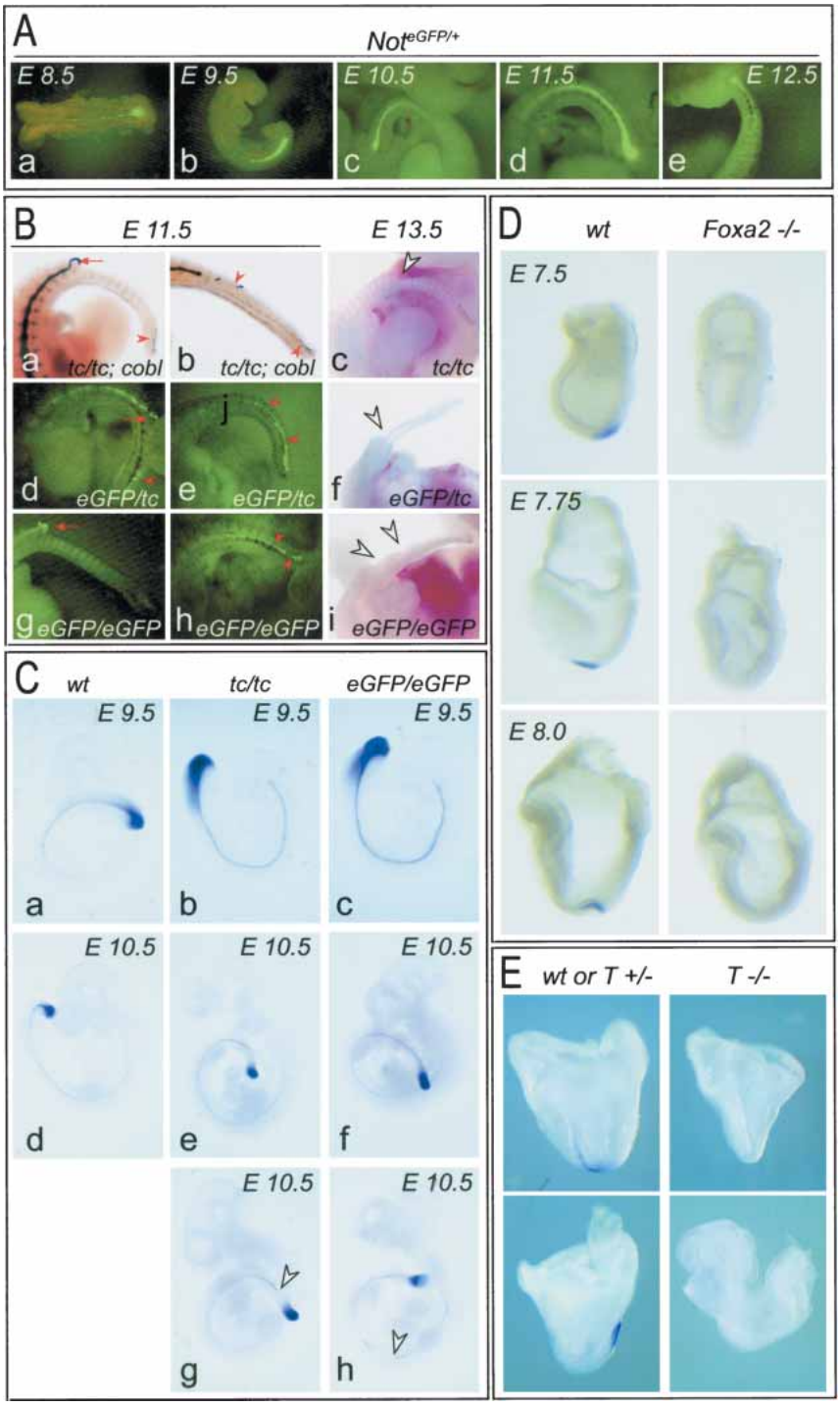

Figure 5. Notochord defects in *Not* mutant embryos and *Not* expression in embryos lacking *Foxa2* or *T* function. (*A*) eGFP expression in heterozygous Not^{eGFP} embryos between day 8.5 and 12.5 of development. (*B*) Notochord and tail defects in $Not^{tc/tc}$ (panels *a–c*), $Not^{eGFP/tc}$ (panels *d–f*), and $Not^{eGFP/eGFP}$ (panels *g–i*), day 11.5 (panels *a*,*b*,*d*,*e*,*g*,*h*) and 13.5 (panels *c*,*f*,*i*) embryos. Arrowheads in panels *c*, *f*, and *i* point to constrictions of the tails. In $Not^{tc/tc}$ day 11.5 embryos, the notochord was visualized by *lacZ* expression from a gene trap insertion into the *Cobl* locus, which was crossed into the mutant background. This insertion leads to *lacZ* expression in the notochord, but does not affect its development (Gasca et al. 1995). In $Not^{tc/eGFP}$ and $Not^{eGFP/eGFP}$ embryos, the notochord phenotype was assessed by eGFP fluorescence. All genotypes showed disruptions of the notochord in and caudal to the sacral region (arrows), or a discontinuous caudal notochord with scattered displaced notochord remnants (arrowheads). (*C*) Brachyury expression in day 9.5 (*a–c*) and 10.5 (*d–h*) wild-type (wt; panels *a*,*d*), $Not^{tc/tc}$ (panels *b*,*e*,*g*), and $Not^{eGFP/eGFP}$ (panels *c*,*f*,*h*) embryos. No notochord defects were observed in day 9.5 embryos. In day 10.5 embryos, notochords were apparently normal (panels *e*,*f*) or showed disruptions in the tail (panel *g*) or trunk region (panel *h*) indicated by arrowheads. (*D*,*E*) Absence of *Not* transcripts in $Foxa2^{-/-}$ (*D*) and $T^{-/-}$ (*E*) embryos.

that Not^{tc} is not a complete null allele. Normal anterior notochord development in both the Not^{eGFP} null and Not^{tc} allele indicates that *Not* function is differentially required along the body axis.

Not *expression requires both* Foxa2 *and* T *function*

To address where in the genetic hierarchy governing notochord formation *Not* might act, we analyzed *Not* expression by whole-mount in situ hybridization in embryos mutant for *Foxa2* and *T*. In the case of *Foxa2*, we used chimeras between homozygous *Foxa2* null ES cells and tetraploid embryos. In these embryos, node and notochord are defective as in *Foxa2* null mutants, but streak morphogenesis is restored (Dufort et al. 1998). No *Not* transcripts were detected in *Foxa2* tetraploid chimeras between E7.5 and E8 (Fig. 5D), suggesting that *Foxa2* is essential for *Not* expression, and thus acts upstream of

Not. Likewise, in 6 of 28 E8–E8.25 embryos obtained from matings between heterozygous *T* mutants, no *Not* transcripts were detected, and in one embryo, *Not* transcripts were severely reduced, whereas the remainder expressed *Not* at indistinguishable levels (Fig. 5E; data not shown), indicating that *T* is also required for *Not* expression, and thus, likely acts upstream of *Not*.

Discussion

We have identified a homeobox gene, which, on the basis of sequence and expression pattern, represents a murine member of the vertebrate *Not* gene family. We have shown by complementation test with a targeted null allele that this gene is affected by the mouse truncate mutation. The phenotype of the Not^{eGFP} null allele indicates that during mouse embryonic development, *Not* function is not essential for anterior notochord formation, suggesting that the genetic control of notochord development in different vertebrate species has diverged.

Relation of mouse Not *to other vertebrate* Not *genes*

The zebrafish *Xenopus* and chicken *Not* genes, whose homeodomains share between 71% and 90% identity, represent a subgroup of the *ems* homeobox gene family (von Dassow et al. 1993; Talbot et al. 1995; Stein et al. 1996). The homeodomain sequence of mouse *Not* has only 56%–60% identical amino acids compared with the other vertebrate *Not* genes, and seems more closely related by sequence to *Emx1/2* and *Drosophila ems.* However, expression in the node, graded expression in the notochord with highest levels posterior, and the requirement of *Not* for notochord development suggest that functionally mouse *Not* represents a new member of the vertebrate *Not* gene family. This is further supported by the results of a phylogenomic approach that led to the identification of mammalian *Not* genes in silico (J.L. Plouhinec, C. Grainier, C. Le Mentec, K.A. Lawson, D. Sabéran-Djoneidi, J. Aghion, D.L. Shi, J. Collignon, and S. Mazan, in prep.). On the basis of sequence similarity, it has been suggested that *Not* genes can be subdivided into two subgroups comprised of *Cnot2/flh* and *Cnot1/Xnot*, respectively (Stein et al. 1996). The murine *Not* homeodomain is most similar to *Cnot2*, suggesting that *Not* constitutes the third member of this group. In addition, the gene structure of *Not* resembles *Cnot2* rather than *Cnot1*, and the expression patterns of *Not* and *Cnot2* appear to be more closely related than expression of *Not* and *Cnot1*, as both *Cnot2* and *Not* lack the limb bud expression domain characteristic for *Cnot1*. It has been suggested that *Cnot2* represents the original gene in chick and *Cnot1*, a duplicated copy, and clustered *Not* homeobox genes are present in all vertebrates (Stein et al. 1996). In mouse, we found no evidence for a second *Not* homeobox gene in the direct vicinity of *Not* or elsewhere in the genome. Likewise, there is no second closely clustered *Not* gene in the zebrafish (http://www.ensembl.org/Danio_rerio) or human (http://www.ensembl.org/Homo_sapiens) genome sequence, suggesting that the tightly clustered *Cnot1* and *Cnot2* genes reflect a gene duplication specific for avians. However, in both the mouse and human genomes, *Emx1* is located ~250 kb next to *Not*. This might indicate that *Not* and *Emx1* represent the results of a gene duplication and diverged with respect to both sequence and regulation, as *Emx1* expression is confined to the dorsal forebrain (Simeone et al. 1992a,b). Thus, the high variability of the *Not* null phenotype cannot be explained by a second *Not* gene, but could be due to another regulatory protein(s) that might partially substitute for *Not* function. Segregating genetic modifiers are less likely to account for this variability, as our analysis was done on a predominantly 129Sv/ImJ background.

The truncate mutation and Not *function*

Lower expression levels of *flh* mRNA in *flh* mutant embryos suggested a positive regulatory effect of *flh* on its own expression (Melby et al. 1997). In contrast, experiments in *Xenopus* embryos have shown that *Xnot1* acts as a transcriptional repressor within the mesodermal region (Yasuo and Lemaire 2001). Temporarily persistent *Not* expression in the head process and anterior notochord of $Not^{tc/tc}$ embryos suggests that *Not* function is required to down-regulate its own expression in the head process/anterior notochord. This is consistent with a repressor function also in mice, although we have not found the conserved eh1 repressor domain (Smith and Jaynes 1996) that was identified in *Xnot1* (Yasuo and Lemaire 2001).

The homeodomain in the truncate allele carries a mutation in helix 1 that changes a conserved hydrophobic amino acid in position 20 of the homeodomain to a polar amino acid. Structural studies have indicated that the primary role of helix 1 and helix 2 is to help stabilize the folded structure of the homeodomain. This stabilization involves a hydrophobic core, to which a conserved Leucine (L16) and Phenylalanine (F20) residue in helix 1 contribute (Qian et al. 1989; Kissinger et al. 1990). The F20C mutation in the truncate allele, which to our knowledge represents the first natural point mutation in the homeodomain of a mouse homeobox gene, leads to a significantly destabilized homeodomain in vitro. Destabilization in vitro, the severe loss-of-function phenotype of Not^{tc} in vivo, and normal notochords in completely ES cell-derived E11.5 $Not^{tc/tcrev}$ embryos, support the significance of hydrophobic interactions between helix 1 and the recognition helix for homeodomain stability, and suggest that F20 is critical for this interaction under physiological conditions in vivo.

The role of Not *in notochord development*

Loss of *Not/flh* function in zebrafish embryos leads to the absence of a differentiated notochord along the entire anterior–posterior body axis (Halpern et al. 1995; Talbot et al. 1995). In *flh* mutant embryos, cells in the position of the notochord express paraxial (muscle) rather than

axial genes, but presumptive notochord cells express properties of axial cells initially (Amacher and Kimmel 1998). This suggests that *flh* is essential for maintaining rather than establishing notochordal fate (Halpern et al. 1995). In *Xenopus* embryos, injection of *Xnot1* or *Xnot2* mRNA resulted in enlarged or multiple notochords (Gont et al. 1996; Yasuo and Lemaire 2001), whereas expression of a VP16-transactivator/XNOT1 homeodomain fusion suppressed notochord formation (Yasuo and Lemaire 2001). Together, the data from studies in *Xenopus* and zebrafish embryos suggested that *Not* genes are necessary and sufficient to maintain notochordal fate in these species and are required along the entire anterior–posterior body axis.

In mouse embryos, the role of *Not* appears to have diverged. Loss of *Not* function does not affect notochord development in the anterior body region, but results in abnormal notochord formation in and caudal to the posterior trunk. This suggests that in mouse embryos, *Not* function is indispensable for notochord development only shortly before and after the tail bud develops and starts to extend the body axis posteriorly. The spatially restricted Not^{eGFP} null phenotype implies regional differences in the genetic control of notochord development in addition to the requirement of increasing brachyury (*T*) levels for notochord formation in the posterior region of the body axis, and identifies *Not* as a critical component contributing to this regionalization.

In homozygous *T* mutant embryos, notochord cells of the head process are formed, but node and trunk notochord are lacking (Herrmann 1995). *Foxa2* mutant embryos lack all notochord cells and an organized node, and express *T* only in cells of the abnormal primitive streak (Ang and Rossant 1994; Weinstein et al. 1994), suggesting that *Foxa2* acts upstream of *T* in notochord cells. The absence of *Not* transcripts in *Foxa2* mutants (Fig. 5D) places *Foxa2* also upstream of *Not*. Loss of *Not* expression in homozygous *T* embryos (Fig. 5E), as well as normal brachyury expression and notochord development in the anterior body region of *Not* mutant embryos (Fig. 5C) suggest that *Not* acts downstream of *T* in notochord cells. Because *Not* expression in the notochord is transient, but *T* expression persists, *T* might be required to initiate *Not* transcription in the notochord and node, but is apparently not sufficient to maintain *Not* expression. Whether *Foxa2* and/or *T* directly regulate *Not* expression remains to be investigated. The action of *Not* downstream of *T* during notochord development in mouse differs from zebrafish. There, *flh* appears to act initially upstream of *T*, as the zebrafish brachyury homolog *ntl* is not expressed in notochord precursors of *flh* mutant embryos (Talbot et al. 1995), and *flh* transcripts are initially present in embryos lacking *ntl* function. At later stages, *ntl* is required to maintain *flh* expression, suggesting that *ntl* and *flh* interact in a regulatory loop (Melby et al. 1997). This lends further support to the notion that the role of *Not* during notochord formation in mouse and zebrafish embryos has diverged.

The notochord in the posterior trunk and tail region of heterozygous *T* embryos is fragmented (Herrmann 1995), closely resembling the *Not* phenotype. Thus, both reduction of *T* or complete loss of *Not* function lead to similar defects. This could be explained by various possible interactions of *T* and *Not*, *T* acts upstream of *Not*, and increasing levels of *T* might be required to activate *Not* in more posterior regions along the body axis. A reduction of *T* would decrease *Not* activity posteriorly below a certain threshold, which in turn would lead to disrupted notochord formation. Alternatively, *T* and *Not* could cooperatively regulate genes critical for posterior notochord formation, and in the posterior region, both high levels of *T* and full function of *Not* are required to maintain notochord development. Either reduction of *T* or loss of *Not* would specifically affect the posterior notochord. In both cases, *T* or another unknown regulatory protein might compensate for loss of *Not* in the anterior notochord. The analysis of double heterozygous *T* and *Not* mutant embryos should help to further elucidate the relation and interaction of *T* and *Not*.

In summary, our analyses support the concept of regional differences in the genetic control of notochord development, and identify *Not* as one important regulator in this process acting downstream of *Foxa2* and *T* during mouse embryonic development. Regionalized control of notochord development also appears to occur in other vertebrate species, as suggested by the zebrafish *mom* mutation, which disrupts notochord formation in the trunk but not in the tail (Odenthal et al. 1996). However, the role of individual components of the genetic hierarchy that governs notochord development appears to vary between different vertebrate species.

Materials and methods

Chromosomal walking

BAC clones were isolated by PCR on BAC DNA pools (Research Genetics 129Sv BAC library) or by hybridization of high-density BAC library filters (C57BL/6; Genome Systems FBAC-4472 and Research Genetics RCPI-22 BAC libraries, respectively). BAC ends were sequenced to generate end-specific hybridization and PCR probes for haplotype analysis of back-cross DNAs, mapping of BAC ends to other BACs, and further library screening. In each walking step, at least two independent BAC clones were analyzed. Their origin from the truncate region was verified by Southern blotting and PCR analyses.

Shotgun cloning and sequencing

Two shotgun libraries of BAC DNA with average insert sizes of 1.5 and 3.5 kb were generated for sequencing. BAC DNA was fragmented by sonication. The resulting fragments were end-repaired, size selected, and ligated into the SmaI-digested and dephosphorylated pUC19 vector (Fermentas). Cloned DNA was electroporated into *Escherichia coli* (strain DH10B; GIBCO), and isolated clones were cultured in 384-well microtiter plates. From each bacterial culture, cloned DNA fragments were amplified by PCR using a modification of the method described by Radelof et al. (1998). DNA was sequenced using BigDye Terminator Chemistry and 3700 ABI capillary sequencer systems (Applera). The quality of raw sequence data was determined with PHRED (Ewing and Green 1998; Ewing et al. 1998). Re-

gions of weak quality within the analyzed contig were resequenced to achieve finished sequence quality of three independent reads of both strands (Hattori et al. 2000). Sequences were then assembled with phrap2gap (http://www.sanger.ac.uk/Software/sequencing/docs/phrap2gap) using PHRAP (Rieder et al. 1998; http://bozeman.genome.washington.edu). GAP4 of the Staden Package (Staden et al. 2000) was used for final editing of the sequence. The nucleotide sequence has been deposited at EMBL under the accession number CR354750. Genes were predicted using ORPHEUS (Frishman et al. 1998). In addition, the nucleotide sequence of the contig was compared with nucleotide databases (EMBL and EMBLNEW) using BLAST algorithms (Altschul et al. 1997). Functional assignment was done with the INTERPRO system (Apweiler et al. 2001). Results from the automated ORF prediction and functional assignment were manually controlled for the entire contig.

Cloning of Not *cDNAs and exons*

Total RNA from wild-type and truncate E9.5 mouse embryos was isolated using the RNeasy Kit (Qiagen). First-strand cDNA was synthesized from 5 µg of total RNA using Superscript II Reverse Transcriptase (Invitrogen) and oligo(dT) primers following the supplier's protocol. PCR (3 min at 94°C, 45 cycles of 30 sec at 94°C, 30 sec at 55°C, 30 sec at 72°C, and final extension at 72°C for 7 min) was performed with primers BG08135F1 (CCTCTCTCTCTCCCATTGAG) and BG08135B10 (CATTTG GTGTCCTTTGACC). PCR products were cloned into pGemTEasy (Promega) and verified by sequencing.

The predicted exons of *Not* were amplified by PCR (3 min at 94°C, 40 cycles of 30 sec at 94°C, 30 sec at 57°C, 30 sec at 72°C, and final extension at 72°C for 7 min) using genomic DNA of wild-type strains (C57BL/6, 129Sv/ImJ, FVB/N, and CD1), and of six homozygous *tc* individuals, respectively, as templates, subcloned into pGemTEasy and sequenced. Primers were Exon1 F2 (CAAGGTCCAGGATAGCCAGAGTTAC) and Exon1 B3 (GGAAAAGTCAGGGGGATGTGAAG) flanking exon1, Exon2 F2 (TTGCTGGCTGAAGTCTGCTCTTGG) and Exon2 B4 (CCA CACACATAAAAAGGAGGAAGC) flanking exon2, and Exon3 F4 (TGTGCGGTGACTGAGAACTTAGG) and Exon3 B6 (TTT GAAGCCAATCTGTGCCAC) flanking exon3.

In situ hybridization

Whole-mount in situ hybridizations were performed following a standard procedure with Digoxygenin-labeled antisense riboprobes (Wilkinson 1992) with minor modifications using an InsituPro (Intavis AG #10.000) for automated liquid handling.

Foxa2 *and* T *mutant embryos*

Foxa2 mutant embryos were obtained by aggregation of tetraploid embryos with homozygous *Foxa2* mutant ES cells (Dufort et al. 1998). *T* mutant embryos were collected from matings between heterozygous brachyury mice carrying the original *T* allele (Dobrovolskaia-Zavadskaia 1927).

Generation of the Not^{eGFP} *allele*

Overlapping DNA fragments of 7.1 and 5.9 kb, respectively, covering ~11.5 kb of the mouse *Not* genomic region were amplified by long-range PCR using the Expand High Fidelity PCR System (Roche) and 129Sv/ImJ genomic DNA as template, and cloned into pCRXL TOPO (Invitrogen). Primer pairs used were F1 (TCCCAGGAACTCAGCGTAG), B1 (TGTTTGCCACATA GCACG), and F2 (CTGTCTTCTGGTTCGGTG), B2 (GTGGCT CACAATCTGTAATG). The translation initiation site in exon 1 was modified by PCR to generate an NcoI restriction site. The eGFP coding region, followed by a SV40 polyadenylation signal was fused in frame to this ATG. Approximately 5 kb of genomic DNA upstream of the ATG, and 4 kb of genomic DNA beginning downstream of exon 2 were included as regions of 5′ and 3′ homology, respectively. A PGKneo cassette flanked by loxP sites was introduced 3′ to the eGFP/SV40pA. To allow for negative selection, a Diphtheria Toxin A expression cassette (pKO SelectDT; Lexicon Genetics) was inserted upstream of the 5′ homology arm (Fig. 1B) in the targeting vector. Linearized vector DNA was electroporated into 129Sv/ImJ ES cells and G41- resistant ES cell clones were selected and expanded essentially as described (Schoor et al. 1999). Correctly targeted clones were identified by PCR using primers derived from the *neo* sequence (F-neo, TGTCACGTCCTGCACGACG), and genomic sequences downstream of the targeting vector (B, CAGCAATCTCTCCAG TTTTTATACG). PCR-positive clones were verified by Southern blot analysis using external probes located 3′ and the 5′ to the regions of homology in the vector (Fig. 4A).

Chimera production and genotyping of mice

For germ-line transmission, ES cells of two independently targeted clones were injected into FVB/N blastocysts that were subsequently transferred to (C57BL/6 × BALBc)F1 pseudopregnant females. Germ-line chimeras were crossed to 129Sv/ImJ females to establish the mutation on an isogenic background. To remove the *neo* cassette, germ-line chimeras were crossed to ZP3::Cre mice (back-cross generation N6 to 129Sv/ImJ) and double heterozygous females bred to wild-type 129Sv/ImJ males. Excision of the neo cassette was ascertained by PCR using the primers Δneo-F (GAGCAAAGACCCCAACGAGAAG) and Δneo-B (GCAACCCACACACATAAAAAGGAG), which gave a PCR product of 420 bp after Cre-mediated recombination. Embryos and mice were genotyped by allele-specific PCR of yolk-sac, tail, or ear punch DNA, respectively, using primers not-F (TGACCACCTCTCTCTCCCATTG) and not-wt-B (CCACCGCTTCCATACTGATACC), detecting a 450-bp fragment indicative for the wild-type allele, and primers not-F and not-GFP-B (TGATGCCGTTCTTCTGCTTGTC), detecting a 552-bp fragment indicative for the mutant allele (Fig. 4B).

Generation of $\text{Not}^{\text{tc/tc}}$ *ES cells and reversion of the* tc *mutation*

ES cells were established from blastocysts obtained from matings between homozygous mutants as described (Maatman et al. 1997). A targeting vector containing ~11 kb of the *Not* locus including the three exons, a Diphtheria Toxin A expression cassette (pKO SelectDT; Lexicon Genetics) upstream of the 5′ homology arm, and a PGKpuro selection cassette flanked by loxP sites in intron 2 (Fig. 3C) was electroporated into truncate ES cells and puromycin resistant ES cell clones were selected and expanded. Correctly targeted clones were identified by PCR using primers derived from the *puro* sequence (puro3′Not-F1, GG GATTAGATAAATGCCTGC), and genomic sequences downstream of the targeting vector (puro3′Not-B2, GAAGAGCCT GACTCAAAAGG). PCR-positive clones were verified by Southern blot analysis using external probes located 3′ and the 5′ to the regions of homology in the vector (Fig. 3C). The *puro* cassette was excised by electroporating ES cells with supercoiled Cre expression plasmid Turbo-Cre (gift of the Embryonic Stem Cell Core of the Siteman Cancer Center, Washington University Medical School), and excision verified by Southern blot hybridization and PCR using primers ca1 (TGACGGAGAATCAG

GTGAGAGCAG) and ca2 (CAACCCACACACATAAAAAGGAGG; Fig. 3C). To generate completely ES cell-derived embryos, ES cells were injected into tetraploid FVB/N morulae that were subsequently transferred to (C57BL/6 × BALBc)F1 pseudopregnant females.

Protein expression and purification

The wild-type and truncate *Not* homeoboxes were amplified from cloned *Not* wild-type and Not^{tc} cDNAs, respectively, using primers not-homeo-F1 (GGGGATCCACAAAGAGGGTTCGCACAACG) and not-homeo-B1 (TTGAATTCTTACAATTTCAGTTTTTGCTGCTTC) and cloned into pGEX6 (Amersham) using the introduced BamHI and EcoRI sites (underlined). Recombinant proteins were expressed and purified as described (Subramaniam et al. 2001).

CD spectroscopy

Circular dichroism measurements were performed in a Jasco J-720 spectropolarimeter (Jasco GmbH) equipped with a Peltier thermostat. The sample concentration (in 10 mM phosphate at pH 7.0, 50 mM NaCl) was determined to be 11 μM. Far UV spectra were run between 197 and 270 nm, in continuous mode, scan speed 50 nm min^{-1}, wavelength step 0.5 nm, spectral resolution 1 nm, integration time 4 sec, T at 4°C. Each run was five times averaged, and the signal arising from the buffer was subtracted from the averaged spectrum. CD data are presented as molecular ellipticity (Θ). Melting curves were obtained by monitoring the ellipticity at 222 nm with a spectral resolution of 2 nm and an integration time of 4 sec. The temperature was scanned at 2°C min^{-1} in the range of 8°C–85°C. No signals of thermal hysteresis were observed. The numerical figures were obtained by fitting a Boltzman curve to the experimental data.

Acknowledgments

We thank Nicholas Willis for excellent technical assistance; Drs. Mazan and Collignon for communicating results prior to publication; Dr. T. Ley and the Embryonic Stem Cell Core of the Siteman Cancer Center, Washington University Medical School, St Louis, MO, for the Turbo-Cre plasmid; and Drs. M. Kessel, A. Kispert, and K. Serth for comments and discussion. This work was supported by a grant from the German Research Council to A.G. (DGF Go449/6-1), and by the German Federal Ministry of Education and Research (BMBF) to R.R. (DHGP-2 Project 01 KW 0001).

The publication costs of this article were defrayed in part by payment of page charges. This article must therefore be hereby marked "advertisement" in accordance with 18 USC section 1734 solely to indicate this fact.

References

Ades, S.E. and Sauer, R.T. 1994. Differential DNA-binding specificity of the engrailed homeodomain: The role of residue 50. *Biochemistry* **33:** 9187–9194.

Altschul, S.F., Madden, T.L., Schaffer, A.A., Zhang, J., Zhang, Z., Miller, W., and Lipman, D.J. 1997. Gapped BLAST and PSI-BLAST: A new generation of protein database search programs. *Nucleic Acids Res.* **25:** 3389–3402.

Amacher, S.L. and Kimmel, C.B. 1998. Promoting notochord fate and repressing muscle development in zebrafish axial mesoderm. *Development* **125:** 1397–1406.

Ang, S.L. and Rossant, J. 1994. HNF-3b is essential for node and notochord formation in mouse development. *Cell* **78:** 561–574.

Apweiler, R., Attwood, T.K., Bairoch, A., Bateman, A., Birney, E., Biswas, M., Bucher, P., Cerutti, L., Corpet, F., Croning, M.D., et al. 2001. The InterPro database, an integrated documentation resource for protein families, domains and functional sites. *Nucleic Acids Res.* **29:** 37–40.

Berry, R.J. 1960. Genetical studies on the skeleton of the mouse XXVI. Pintail. *Genet. Res. Camb.* **1:** 439–451.

Bumcrot, D.A. and McMahon, A.P. 1995. Somite differentiation. Sonic signals somites. *Curr. Biol.* **5:** 612–614.

de Vries, W.N., Binns, L.T., Fancher, K.S., Dean, J., Moore, R., Kemler, R., and Knowles, B.B. 2000. Expression of Cre recombinase in mouse oocytes: A means to study maternal effect genes. *Genesis* **26:** 110–112.

Dietrich, S., Schubert, F.R., and Gruss, P. 1993. Altered Pax gene expression in murine notochord mutants: The notochord is required to initiate and maintain ventral identity in the somite. *Mech. Dev.* **44:** 189–207.

Dobrovolskaia-Zavadskaia, N. 1927. Sur al mortification spontanée dela queue chez la souris nouveau-née et sur l'existence d'uncaracére hereditaire 'non viable'. *C.R. Soc. Biol.* **97:** 114–116.

Dufort, D., Schwartz, L., Harpal, K., and Rossant, J. 1998. The transcription factor HNFβ is required in visceral endoderm for normal primitive streak morphogenesis. *Development* **125:** 3015–3025.

Echelard, Y., Epstein, D.J., St Jacques, B., Shen, L., Mohler, J., McMahon, J.A., and McMahon, A.P. 1993. Sonic hedgehog, a member of a family of putative signaling molecules, is implicated in the regulation of CNS polarity. *Cell* **75:** 1417–1430.

Ewing, B. and Green, P. 1998. Base-calling of automated sequencer traces using phred. II. Error probabilities. *Genome Res.* **8:** 186–194.

Ewing, B., Hillier, L., Wendl, M.C., and Green, P. 1998. Base-calling of automated sequencer traces using phred. I. Accuracy assessment. *Genome Res.* **8:** 175–185.

Frishman, D., Mironov, A., Mewes, H.W., and Gelfand, M. 1998. Combining diverse evidence for gene recognition in completely sequenced bacterial genomes. *Nucleic Acids Res.* **26:** 2941–2947.

Gasca, S., Hill, D.P., Klingensmith, J., and Rossant, J. 1995. Characterization of a gene trap insertion into a novel gene, cordon-bleu, expressed in axial structures of the gastrulating mouse embryo. *Dev. Genet.* **17:** 141–154.

Gluecksohn-Schoenheimer, S. 1943. The morphological manifestations of a dominant mutation in mice affecting tail and urogenital system. *Genetics* **28:** 341–348.

Gont, L.K., Steinbeisser, H., Blumberg, B., and de Robertis, E.M. 1993. Tail formation as a continuation of gastrulation: The multiple cell populations of the *Xenopus* tailbud derive from the late blastopore lip. *Development* **119:** 991–1004.

Gont, L.K., Fainsod, A., Kim, S.H., and De Robertis, E.M. 1996. Overexpression of the homeobox gene Xnot-2 leads to notochord formation in *Xenopus*. *Dev. Biol.* **174:** 174–178.

Halpern, M.E., Thisse, C., Ho, R.K., Thisse, B., Riggleman, B., Trevarrow, B., Weinberg, E.S., Postlethwait, J.H., and Kimmel, C.B. 1995. Cell-autonomous shift from axial to paraxial mesodermal development in zebrafish floating head mutants. *Development* **121:** 4257–4264.

Hattori, M., Fujiyama, A., Taylor, T.D., Watanabe, H., Yada, T., Park, H.S., Toyoda, A., Ishii, K., Totoki, Y., Choi, D.K., et al. 2000. The DNA sequence of human chromosome 21. *Nature* **405:** 311–319.

Herrmann, B.G. 1995. The mouse *Brachyury* (*T*) gene. *Sem. Dev. Biol.* **6:** 385–394.

Herrmann, B.G., Labeit, S., Poustka, A., King, T.R., and Lehrach, H. 1990. Cloning of the *T* gene required in mesoderm formation in the mouse. *Nature* **343:** 617–622.

Kinder, S.J., Tsang, T.E., Wakamiya, M., Sasaki, H., Behringer, R.R., Nagy, A., and Tam, P.P. 2001. The organizer of the mouse gastrula is composed of a dynamic population of progenitor cells for the axial mesoderm. *Development* **128:** 3623–3634.

Kissinger, C.R., Liu, B.S., Martin-Blanco, E., Kornberg, T.B., and Pabo, C.O. 1990. Crystal structure of an engrailed homeodomain–DNA complex at 2.8 A resolution: A framework for understanding homeodomain–DNA interactions. *Cell* **63:** 579–590.

Lawson, K.A. and Pedersen, R.A. 1992. Clonal analysis of cell fate during gastrulation and early neurulation in the mouse. *Ciba Found. Symp.* **165:** 3–21.

Lawson, K.A., Meneses, J.J., and Pedersen, R.A. 1991. Clonal analysis of epiblast fate during germ layer formation in the mouse embryo. *Development* **113:** 891–911.

Maatman, R., Zachgo, J., and Gossler, A. 1997. The Danforth's short tail mutation acts cell autonomously in notochord cells and ventral hindgut endoderm. *Development* **124:**4019–4028.

Melby, A.E., Kimelman, D., and Kimmel, C.B. 1997. Spatial regulation of floating head expression in the developing notochord. *Dev. Dyn.* **209:** 156–165.

Nagy, A., Gocza, E., Diaz, E.M., Prideaux, V.R., Ivanyi, E., Markkula, M., and Rossant, J. 1990. Embryonic stem cells alone are able to support fetal development in the mouse. *Development* **110:** 815–821.

Odenthal, J., Haffter, P., Vogelsang, E., Brand, M., van Eeden, F.J., Furutani-Seiki, M., Granato, M., Hammerschmidt, M., Heisenberg, C.P., Jiang, Y.J., et al. 1996. Mutations affecting the formation of the notochord in the zebrafish, Danio rerio. *Development* **123:** 103–115.

Pavlova, M.N., Clark, A.M., and Gossler, A. 1998. High-resolution mapping of the truncate (tc) locus on mouse Chromosome 6. *Mamm. Genome* **9:** 843–845.

Placzek, M., Tessier-Lavigne, M., Yamada, T., Jessell, T., and Dodd, J. 1990. Mesodermal control of neural cell identity: Floor plate induction by the notochord. *Science* **250:** 985–988.

Pourquié, O., Coltey, M., Teillet, M.A., Ordahl, C., and Le Douarin, N.M. 1993. Control of dorsoventral patterning of somitic derivatives by notochord and floor plate. *Proc. Natl. Acad. Sci.* **90:** 5242–5246.

Qian, Y.Q., Billeter, M., Otting, G., Muller, M., Gehring, W.J., and Wuthrich, K. 1989. The structure of the Antennapedia homeodomain determined by NMR spectroscopy in solution: Comparison with prokaryotic repressors. *Cell* **59:** 573–580.

Radelof, U., Hennig, S., Seranski, P., Steinfath, M., Ramser, J., Reinhardt, R., Poustka, A., Francis, F., and Lehrach, H. 1998. Preselection of shotgun clones by oligonucleotide fingerprinting: An efficient and high throughput strategy to reduce redundancy in large-scale sequencing projects. *Nucleic Acids Res.* **26:** 5358–5364.

Rieder, M.J., Taylor, S.L., Tobe, V.O., and Nickerson, D.A. 1998. Automating the identification of DNA variations using quality-based fluorescence re-sequencing: Analysis of the human mitochondrial genome. *Nucleic Acids Res.* **26:** 967–973.

Schoenwolf, G.C. 1984. Histological and ultrastructural studies of secondary neurulation in mouse embryos. *Am. J. Anat.* **169:** 361–376.

Schoor, M., Schuster-Gossler, K., Roopenian, D., and Gossler, A. 1999. Skeletal dysplasias, growth retardation, reduced postnatal survival, and impaired fertility in mice lacking the SNF2/SWI2 family member ETL1. *Mech. Dev.* **85:** 73–83.

Selleck, M.A. and Stern, C.D. 1991. Fate mapping and cell lineage analysis of Hensen's node in the chick embryo. *Development* **112:** 615–626.

Simeone, A., Acampora, D., Gulisano, M., Stornaiuolo, A., and Boncinelli, E. 1992a. Nested expression domains of four homeobox genes in developing rostral brain. *Nature* **358:** 687–690.

Simeone, A., Gulisano, M., Acampora, D., Stornaiuolo, A., Rambaldi, M., and Boncinelli, E. 1992b. Two vertebrate homeobox genes related to the *Drosophila* empty spiracles gene are expressed in the embryonic cerebral cortex. *EMBO J.* **11:** 2541–2550.

Smith, S.T. and Jaynes, J.B. 1996. A conserved region of engrailed, shared among all en-, gsc-, Nk1-, Nk2- and msh-class homeoproteins, mediates active transcriptional repression in vivo. *Development* **122:** 3141–3150.

Staden, R., Beal, K.F., and Bonfield, J.K. 2000. The Staden package, 1998. *Methods Mol. Biol.* **132:** 115–130.

Stein, S. and Kessel, M. 1995. A homeobox gene involved in node, notochord and neural plate formation of chick embryos. *Mech. Dev.* **49:** 37–48.

Stein, S., Niss, K., and Kessel, M. 1996. Differential activation of the clustered homeobox genes CNOT2 and CNOT1 during notogenesis in the chick. *Dev. Biol.* **180:** 519–533.

Subramaniam, V., Jovin, T.M., and Rivera-Pomar, R.V. 2001. Aromatic amino acids are critical for stability of the bicoid homeodomain. *J. Biol. Chem.* **276:** 21506–21511.

Talbot, W.S., Trevarrow, B., Halpern, M.E., Melby, A.E., Farr, G., Postlethwait, J.H., Jowett, T., Kimmel, C.B., and Kimelman, D. 1995. A homeobox gene essential for zebrafish notochord development. *Nature* **378:** 150–157.

Tam, P.P., Steiner, K.A., Zhou, S.X., and Quinlan, G.A. 1997. Lineage and functional analyses of the mouse organizer. *Cold Spring Harb. Symp. Quant. Biol.* **62:** 135–144.

Theiler, K. 1959. Anatomy and development of the 'truncate' (boneless) mutation in the mouse. *Am. J. Anat.* **104:** 319–343.

———. 1988. *Vertebral malformations*. Springer Verlag, Berlin, Heidelberg, New York.

van Straaten, H.W. and Hekking, J.W. 1991. Development of floor plate, neurons and axonal outgrowth pattern in the early spinal cord of the notochord-deficient chick embryo. *Anat. Embryol. Berl.* **184:** 55–63.

van Straaten, H.W.M., Thors, F., Wiertz-Hoessels, L., Hekking, J., and Drukker, J. 1985. Effect of a notochordal implant on the early morphogenesis of the neural tube and neuroblasts: Histometrical and histological results. *Dev. Biol.* **110:** 247–254.

von Dassow, G., Schmidt, J.E., and Kimelman, D. 1993. Induction of the *Xenopus* organizer: Expression and regulation of Xnot, a novel FGF and activin-regulated homeo box gene. *Genes & Dev.* **7:** 355–366.

Weinstein, D.C., Ruiz i Altaba, A., Chen, W.S., Hoodless, P., Prezioso, V.R., Jessell, T.M., and Darnell Jr., J.E. 1994. The winged-helix transcription factor HNF-3 β is required for notochord development in the mouse embryo. *Cell* **78:** 575–588.

Wilkinson, D.G. 1992. Whole mount in situ hybridization of vertebrate embryos. In *In situ hybridization: A practical approach* (ed. D.G. Wilkinson), pp. 75–84. Oxford University Press, Oxford, UK.

Wilson, V. and Beddington, R.S.P. 1996. Cell fate and morphogenetic movement in the late mouse primitive streak. *Mech. Dev.* **55:** 79–89.

Yamada, T., Placzek, M., Tanaka, H., Dodd, J., and Jessell, T.M. 1991. Control of cell pattern in the developing nervous system: Polarizing activity of the floor plate and notochord. *Cell* **64:** 635–647.

Yasuo, H. and Lemaire, P. 2001. Role of Goosecoid, Xnot and Wnt antagonists in the maintenance of the notochord genetic programme in *Xenopus* gastrulae. *Development* **128:** 3783–3793.

The mouse homeobox gene *Not* is required for caudal notochord development and affected by the truncate mutation

Hanaa Ben Abdelkhalek, Anja Beckers, Karin Schuster-Gossler, et al.

Genes Dev. 2004 18: 1725-1736
Access the most recent version at doi:10.1101/gad.303504